Konya Mühendislik Bilimleri Dergisi, c. 12, s. 2, 307-325, 2024
Konya Journal of Engineering Sciences, v. 12, n. 2, 307-325, 2024
ISSN: 2667-8055 (Electronic)
DOI: 10.36306/konjes.1398634

EFFECT OF PILE GEOMETRY AND SOIL SATURATION DEGREE ON POINT BEARING CAPACITY FOR BORED PILES IN SANDS

[1,*] Yavuz YENGİNAR, [2] Bekir FİDAN, [3] Murat OLGUN

[1] *Necmettin Erbakan University, Engineering Faculty, Civil Engineering Department, Konya, TÜRKİYE*
[2] *Ministry of Interior Disaster and Emergency Management Presidency (AFAD) Konya Provincial Directorate of Disaster and Emergency, Konya, TÜRKİYE*
[3] *Konya Technical University, Engineering and Natural Sciences Faculty, Civil Engineering Department, Konya, TÜRKİYE*
[1] yyenginar@erbakan.edu.tr, [2] bekirfidann@gmail.com, [3] molgun@ktun.edu.tr

Highlights

- Loading speed does not affect the ultimate point and total bearing capacities of the pile significantly.
- The base, shaft, and total bearing capacities of piles mobilized at different settlement values.
- The base and total capacities of piles decrease 65 to 75% when the dry soil becomes saturated.
- Experimental Nq coefficients were smaller than coefficients of Vesic and Meyerhof but closer to Janbu's.
- Nq value depends on the internal friction angle of soil, effective stress, pile diameter, and saturation degree.
- In dry and saturated sands, Nq value decreases since the pile length/pile diameter ratio increases.

Graphical Abstract

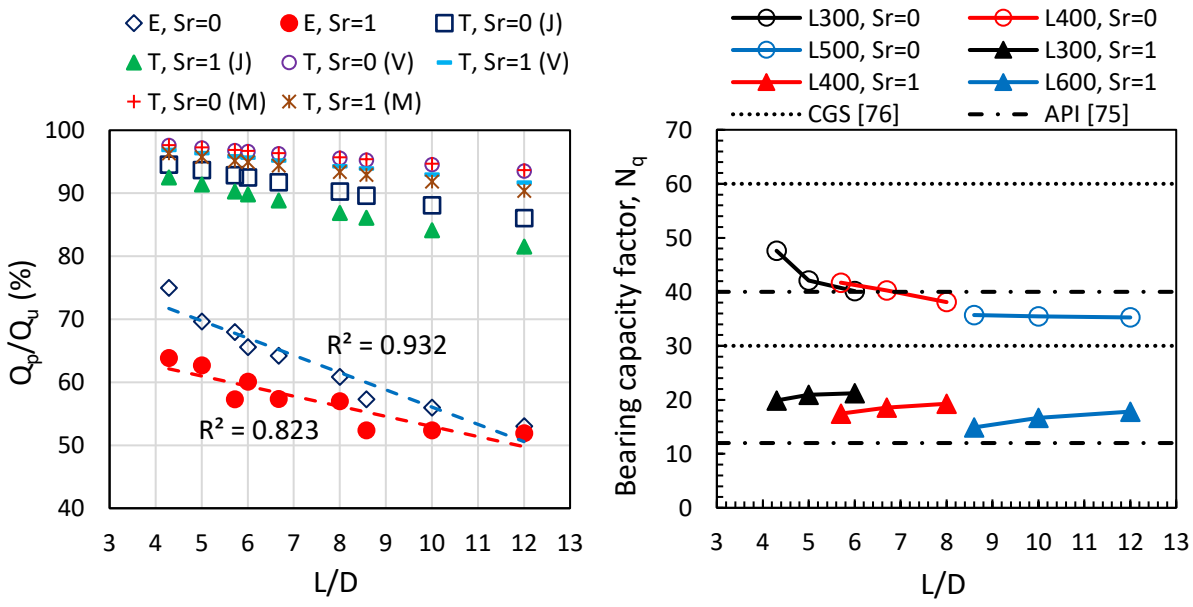

The percentage of point capacity in ultimate bearing capacity (left) and the variation of Nq values depending on L/D (right)
(Q_p: point capacity, Q_u: ultimate capacity, L: pile length, D: pile diameter, Sr: saturation degree of soil, E: experimental, T: theoretical, J: Janbu, V: Vesic, M: Meyerhof,)

*Corresponding Author: Yavuz YENGİNAR, yyenginar@erbakan.edu.tr

Konya Mühendislik Bilimleri Dergisi, c. 12, s. 2, 307-325, 2024
Konya Journal of Engineering Sciences, v. 12, n. 2, 307-325, 2024
ISSN: 2667-8055 (Electronic)
DOI: 10.36306/konjes.1398634

EFFECT OF PILE GEOMETRY AND SOIL SATURATION DEGREE ON POINT BEARING CAPACITY FOR BORED PILES IN SANDS

[1,*] Yavuz YENGİNAR, [2] Bekir FİDAN, [3] Murat OLGUN

[1] *Necmettin Erbakan University, Engineering Faculty, Civil Engineering Department, Konya, TÜRKİYE*
[2] *Ministry of Interior Disaster and Emergency Management Presidency (AFAD) Konya Provincial Directorate of Disaster and Emergency, Konya, TÜRKİYE*
[3] *Konya Technical University, Engineering and Natural Sciences Faculty, Civil Engineering Department, Konya, TÜRKİYE*
[1] yyenginar@erbakan.edu.tr, [2] bekirfidann@gmail.com, [3] molgun@ktun.edu.tr

(Received: 30.11.2023; Accepted in Revised Form: 24.02.2024)

ABSTRACT: In the present paper, an experimental study was conducted to determine the factors affecting the point bearing capacity of pile foundations constructed in dry and saturated sandy soils. Model piles were installed as reinforced concrete bored piles cast-in-situ. Model pile foundations of various geometries resting at different depths in homogeneous sand of different saturation degrees (%0-100) were loaded statically to failure. The test results showed that the bearing capacity of piles did not significantly affect by the loading rate. At most 10% difference was observed in pile bearing capacity when the loading rate was between 0.7 and 2.5 mm/min. Subsequently, the load bearing capacities of the piles were determined at a specified constant loading rate. The point and total capacities of the piles were measured separately in the experiments, then test results were compared with theoretical values. Pile point capacities provided from pile load tests are smaller than the theoretical values. The differences between experimental and theoretical results have been attributed to the N_q values. The N_q values not only dependent on the internal friction angle of the soil but also the saturation degree of the soil, the pile diameter, and the effective stress. N_q values decrease since the pile length/pile diameter ratio increases.

Keywords: *Bearing Capacity Factor, Pile Load Test, Point Resistance, Sand, Saturation Degree, Single Pile*

1. INTRODUCTION

Pile foundations are the most preferred practices in solving the foundation problems, such as bearing capacity, settlement, stability problems, liquefaction, and groundwater flow. In field applications, pile foundations are manufactured for soldier piles (lateral loaded piles) [1], [2] or soil reinforcement piles (vertical loaded piles) [3], [4], [5]. In soil reinforcement works, more than one pile is manufactured according to the project requirements, and the piles are ensured to carry the load as a group. If a raft plate is manufactured on the pile group, the system becomes a piled raft. In the pile foundation systems (single pile, pile group, and pile raft), the load-bearing capacity and load-settlement behavior of each pile are different [6]. The piled raft system is mostly used in soil reinforcement works and the load transfer mechanism between the pile-soil-raft is very complex [6], [7], [8]. If the load-settlement behavior of single piles can be determined accurately, it will enable more reliable designs of pile groups and piled rafts.

Pile foundations are classified as point bearing or friction piles according to the mechanisms of load transfer. The total bearing capacity of the pile is mostly met by the shaft capacity in friction piles and by the point capacity in the point bearing piles [9], [10]. However, the point capacity of piles installed in sandy soil constitutes a significant portion of the pile bearing capacity [11], [12], [13], [14]. Point and shaft capacities are not independent of one another because improving the load-bearing layer at the pile base is not only increases point capacity but at the same time improves the shaft capacity [15].

The soil properties (soil type, shear strength parameters), pile material type (steel, concrete, wood), the construction method (driven or bored piles), the loading direction (axial or lateral), and groundwater

*Corresponding Author: Yavuz YENGİNAR, yyenginar@erbakan.edu.tr

conditions (effective stress and pore water pressure) have decisive effects on the load-settlement characteristics of pile. There are still some uncertainties on the pile behavior since many factors affect the pile-soil interactions. In the last decade, empirical or semi-empirical methods enhanced to determine the load transfer mechanism of bored piles [16], [17], [18], [19], [20]. In addition, some analytical models have been developed to estimate pile capacity considering the pile diameter, soil properties, and stress in soil body [21], [22], [23], [24], [25], [26]. In non-displacement piles, Han et al. [27] reported that increments of relative density of sand and lateral stress at pile base increase the ultimate base resistance but pile diameter has no effect on base resistance.

The bearing capacity factor (N_q) is the most important parameter affecting the pile point resistance. N_q values usually get constant values according to the internal friction angle of the soil (ϕ). Many researchers have developed equations or graphs for the N_q coefficient depending on the ϕ [28], [29], [30], [31], [32], [33]. Cheng [34] proposed to increase the N_q values developed by Berezantzev [28] by 4 to 10%.

The pile point resistance also increases by the effective stress in soil body. However, pile load tests in the field cases indicate that a linear increase was not observed on point resistance, depending on the effective stress in soil. Consequently, the expression of "limit point pressure" to limit the point resistance has been developed [31], [35]. The limitation of the point resistance is caused by the arching and clamping effects occurring in the soil. The pile point resistance increases with depth at a gradually decreasing rate and it is stated that there is no limit value [28], [29], [36], [37]. Meyerhof [38] and Bolton [39] reported that the main reason for the decrease in "the amount of increase in the point resistance" is the reduction in the internal friction angle of the soil because of increasing confining pressure with depth.

The groundwater level may change depending on the seasonal conditions. This situation affects the bearing capacity of pile foundations and may lead to an increase in settlement. Studies, where groundwater level has been taken into account, are generally on structures manufactured on the seashore or offshore and are mostly performed on driven steel piles [40], [41], [42], [43], [44]. Very few studies investigated the load-settlement behavior of bored (nondisplacement) piles in saturated soils. Nguyen et al. [45] reported that as a result of the lowering of groundwater, the bending moments on piles and the amount of settlement are increasing and then structural damage occurs. Sheikhtaheri [46] stated that the point and shaft capacities of the piles in saturated sandy soil decrease by 2-2.5 and 5 times, respectively, as compared with the piles installed in non-saturated soil. Olgun et al. [47] reported that the pile shaft capacity decreases by 55.7% to 68.2% depending to pile length/diameter ratio when groundwater level rises. Mukhlisin *et al*. [48] stated that increasing soil moisture content cause a decrease in friction resistance. Pile shaft capacity decreases when groundwater level increases since effective stress in soil mass decreases [49], [50]. Chong and Ong [51] observed relatively large settlements in contiguous bored pile due to the sudden decrease of groundwater during tunnel construction. In addition, axial force on the pile increases due to the negative skin friction if settlement of soil is more than pile settlement during groundwater lowering [52]. This phenomenon decreases the pile bearing capacity [53].

In this study, model piles have diameters of 50-60-70 mm and lengths of 300-400-600 mm were installed in sandy soil. Thus, piles similar to one in the field are modeled in the laboratory. Firstly, a model pile loaded in nine different loading rates (between 0.7 and 2.5 mm/min) and the differences in bearing capacity were investigated. Subsequently, the load-settlement behaviors of the model piles constructed in dry and saturated sandy soils having the same void ratio were investigated with constant penetration load tests. In the tests, the point and total bearing capacities of the piles were measured separately. The effect of the soil saturation degree, pile length, and pile diameter on the point and total bearing capacities of piles were investigated. This study is an extended version of the previous study [54], in which only the load-bearing capacity of the pile base was investigated. The novel approaches of this study are model piles have more realistic surface roughness since they are manufactured as cast-in-place reinforced concrete, load-settlement values of the pile base are measured directly, pile loading tests carried out in a large-scale test setup, and groundwater effect is included.

2. PILE BEARING CAPACITY

The ultimate load capacity of the pile can be determined with the following equation:

$$Q_u = Q_f + Q_p \tag{1}$$

where; Q_u=ultimate pile capacity in compression, Q_f=ultimate load capacity of pile shaft, Q_p=ultimate load capacity of the pile point.

2.1 Point Capacity

Generally, the point capacity of piles installed in sandy soil could be found by the following relationship [31]:

$$Q_p = \sigma' N_q A_p \tag{2}$$

where; σ'=effective vertical stress at the level of pile end, N_q=bearing capacity factor, A_p=area of pile point.

The N_q value suggested by Vesic [33] and Janbu [30] is given in Eq. 3 and Eq. 4, respectively. Meyerhof [55] developed a graphical chart for N_q values depending on ϕ (Figure 13), but there is no analytical formula.

$$N_q = \frac{3}{3-\sin\phi}\left\{exp\left[\left(\frac{\pi}{2}-\phi\right)\tan\phi\right]\tan^2\left(45^0+\frac{\phi}{2}\right) Irr^{\frac{1.333\sin\phi}{1+\sin\phi}}\right\} \tag{3}$$

$$N_q = \left(\tan\phi + \sqrt{1+\tan^2\phi}\right)^2 exp(2\psi\tan\phi) \tag{4}$$

where; I_{rr}=reduced rigidity index ($I_{rr} = I_r/(1 + I_r\Delta)$), I_r=rigidity index (for sand 75-150), Δ=average volumetric strain in the plastic zone below the pile point, ψ angle is given in Figure 1 and changes between 60° (loose sand) and 105º (dense sand).

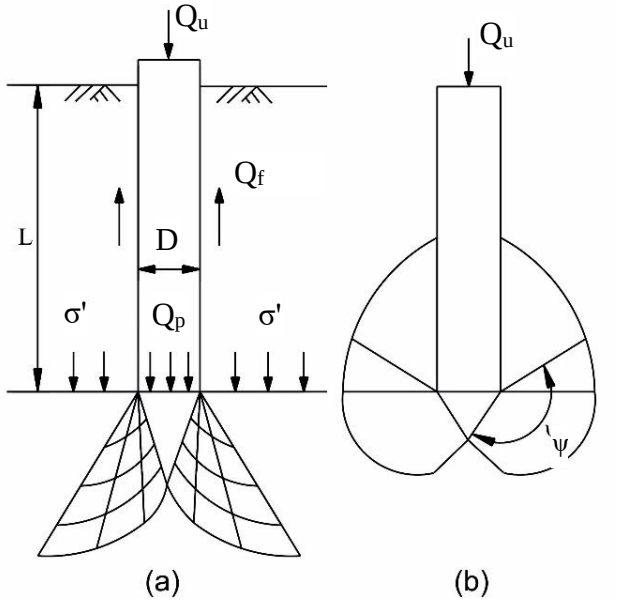

Figure 1. The shear surfaces at the pile point at failure a) Vesic, b) Janbu, and Meyerhof [56]

Equation (2) indicates that the pile point capacity increases linearly depending on the effective stress since N_q and A_p have constant values according to soil and pile properties, respectively. However, Vesic [33] stated that due to the coupling effect on the soil after a depth of 20D, the pile point capacity remains constant. In addition, critical pile depth (L_{cr}) is recommended as 10D, 15D, and 20D for loose, medium dense, and dense sands, respectively [57]. Poulos and Davis [35] defined the L_{cr} depending on the internal friction angle as follows:

$$L_{cr}/D = 5 + 0.24(\phi - 28) \quad 28<\phi<36.5 \tag{5}$$
$$L_{cr}/D = 7 + 2.35(\phi - 36.5) \quad 36.5<\phi<42 \tag{6}$$
$$\phi = \phi_1 - 3 \quad \text{for bored piles} \tag{7}$$

where; L_{cr}=critical depth, D=pile diameter, ϕ_1=angle of internal friction prior to the installation of the pile

2.2 Shaft Capacity

Burland [58] has proposed the following relationship for piles installed in sandy soil for shaft capacity:

$$Q_f = \beta \cdot \sigma_o' \cdot A_s \tag{8}$$
$$\beta = K \cdot tan\,\delta \tag{9}$$

where; σ_o' =average effective vertical stress, K=the lateral earth pressure coefficient, δ=effective friction angle between soil and pile material, A_s=pile surface area

The shaft capacity increases linearly but the shaft capacity remains constant, as with the pile point capacity, after a critical depth (15D) [10].

3. EXPERIMENTAL SETUP

The experimental setup has a model tank box or container, a loading frame, a hydraulic piston, hydraulic control unit, and data acquisition unit, load cells, and dial gauges (Figure 2). Diameter and height of the model tank are 65 cm and 110 cm, respectively. The hydraulic loading unit, which has 100 kN-capacity, is fixed to the upper part of the loading frame. The loading speed of the piston can be adjusted from a hydraulic control unit. The load and settlement values measured during the test are recorded by a software with the help of a data collection unit.

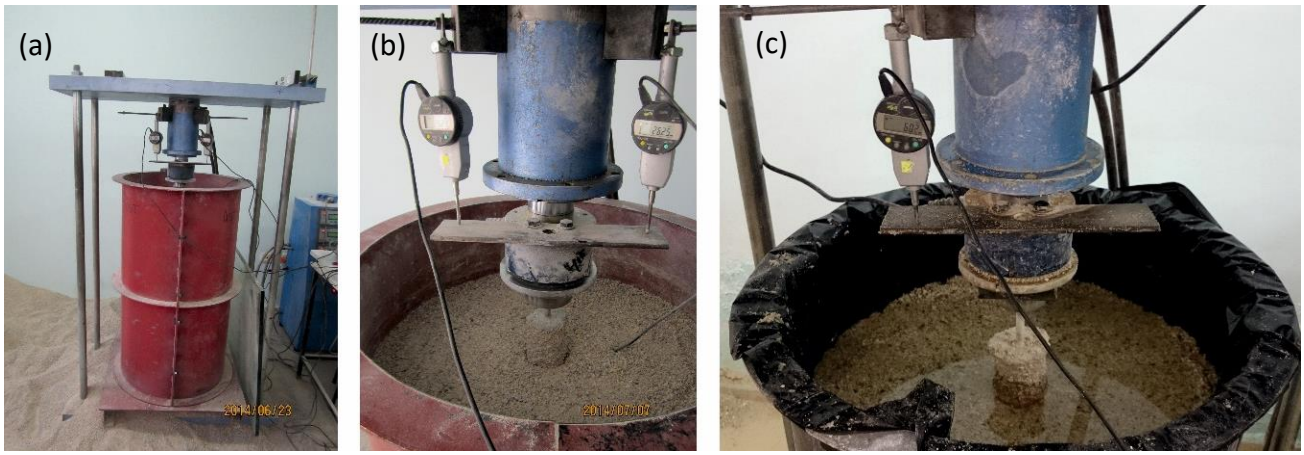

Figure 2. a) The general view of pile loading experimental setup on condition of b) S_r=0 and c) S_r=1

3.1 Geotechnical Properties of Soil

Sandy soil was used in the model pile loading tests. The sandy soil contains 44% coarse sand, 47% medium sand, and 9% fine sand (Figure 3). Sandy soil is classified as SP (poorly graded sand) according to USCS [59]. The geotechnical properties of the sand were given in Table 1. In the pile loading experiments, dry and saturated sandy soil masses having same void ratio were placed into the tank. The relative density of the soil was 39.4% by ASTM D4254-1 [60]. Internal friction angles of the soils were determined to be 37.2° and 34.5° in dry and saturated states, respectively, resulting from shear box tests [61].

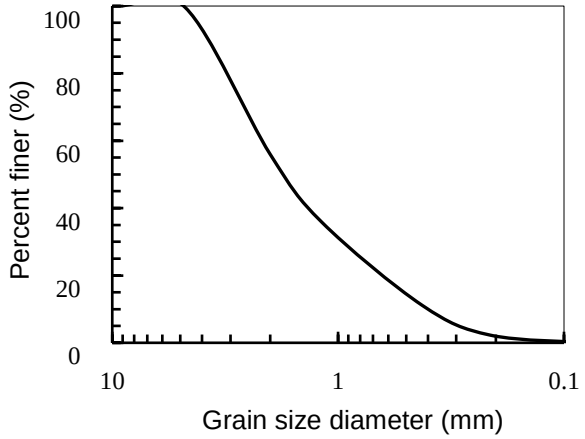

Figure 3. Grain size distribution of soil

Table 1. Geotechnical properties of sand

Coefficient of uniformity	C_u	4.87
Coefficient of curvature	C_c	1.09
Unit weight of soil particles	γ_s (kN/m^3)	26.20
Dry unit weight	γ_d (kN/m^3)	16.37
Saturated unit weight	γ_{sat} (kN/m^3)	20.05
Maximum void ratio	e_{max}	0.730
Minimum void ratio	e_{min}	0.400

3.2 Construction of Model Piles

Model piles were manufactured as cast in-situ, reinforced concrete, and bored piles in the laboratory. During the pile installation process, casing pipes were used because the piles were manufactured in cohesionless soil. Firstly, the model container or box was filled with some amount of sand and then casing pipes were placed vertically on the sand surface. After that, the remaining part of the tank between the casing pipes was filled with sandy soil. Before the concreting process, a 12 mm diameter threaded rod was placed at the center of the casing pipe vertically. The threaded rod has been used for the reinforcement function and mounting the s-type load cell to the pile bottom. In the pile loading experiments, pile base capacity is measured directly by the virtue of load cell. During the concreting process, the piles were created by pulling up the casing pipe simultaneously (Figure 4a). Piles were being left two days in the soil to gain resistance against breakage (Figure 4b). After two days, the model piles were removed from the soil environment and they were cured in the curing pool for seven days to gain enough strength. The pile surface roughness and pile-soil interaction are provided to be similar to the field conditions by manufacturing model piles using this technique (Figure 4c). Constructed piles had diameters (D) of 50-60-

70 mm and lengths (L) of 300-400-600 mm and they were been named by diameter-length (D70L600, D50L300…).

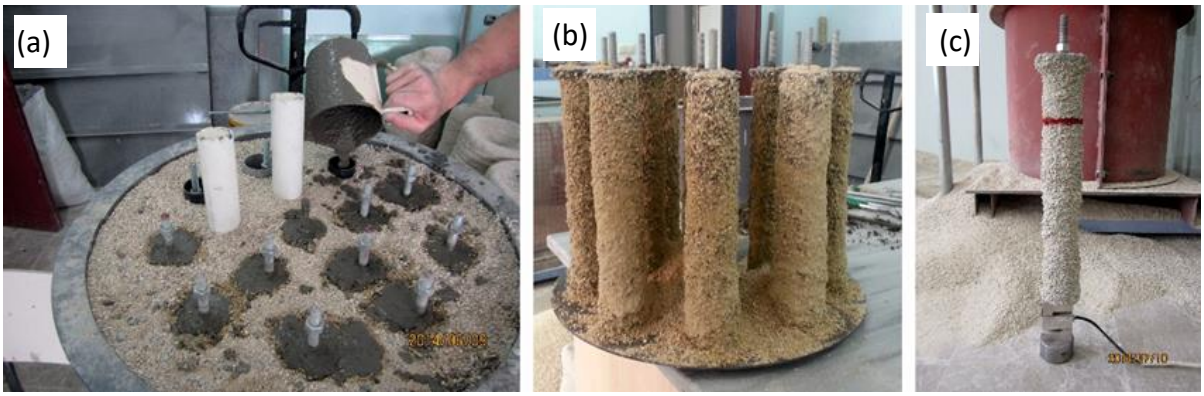

Figure 4. a, b) Construction of the piles in sandy soil, c) a model pile

3.3 Test Program and Methods

One of the aims of this study is to determine the changes in the pile bearing capacity due to changes in groundwater level. For this reason, in the model pile loading experiments, the soil condition must be in the same void ratio in dry and saturated conditions. The void ratio of dry and saturated soil mass is 0.6 (Dr=39.4%). In order to obtain same void ratio for both soil state, the mass of the soil at a certain height was determined using the grain density and dry/saturated unit weight properties of the soil. Then, the materials were weighed and placed in the tank. In the experiments performed in the dry state, the sand inside a funnel was always dropped from the same height (pluviation technique), flowing by its weight, into the test tank. In the experiments performed in saturated sand, the soil was placed into the test tank by tamping, laying, and compressing layer by layer. Compacting energy applied to soil (hammer weight, number of blows, and height of drop) was arranged to obtain the same void ratio with the sand of dry state. Before loading the model piles, static groundwater level raised up to soil surface and all voids between soil grains filled with water. To prevent water infiltration, a seamless plastic bag was used in experiments on saturated sandy soils (Figure 2c). In both soil conditions, the distance between pile end and bottom of the test tank is 40-70 cm (5.7D-10D) and 28-30 cm (3.8D-5.5D) from the tank surface to the pile surface (Figure 5a). Minimum distance between pile and container boundary is required 2.5D along the horizontal direction and 4D along the vertical direction for axial loading, where D is the pile diameter [62], [63]. In addition, D70L600 pile is modelled in Plaxis 3D software, and the stress at the container boundary is close to 0 kPa when the pile is loaded at ultimate capacity (2.36 kN or 653 kPa) (Figure 5b). The adequate distance between pile and tank surface exists in the model tests. Therefore, the stresses transferred from the pile to the soil do not reach the tank boundary.

The load-settlement behavior of the model piles was determined by loading the piles with a load larger than the failure load. That is, model piles were loaded until 40 mm settlement amount at which they were already reached to failure load. The ultimate pile capacity (Q_u) was measured with the total load applied from hydraulic piston. The load transferred to the pile end was measured by the load cell mounted to pile bottom, which gave the pile point capacity (Q_p). The pile shaft capacity (Q_f) was the difference between total and point capacities of the model pile. During the pile loading experiment, Q_p, Q_u and settlement (ΔH) values were recorded through the data acquisition system. After drawing the Q_p-ΔH and Q_u-ΔH curves, the limit values of Q_p and Q_u were determined by the tangent method [64]. In this method, the intersection points of the tangent lines drawn at the beginning and end parts of the load-settlement curve gives the limit load. The pile is mobilized at the settlement value corresponding to the limit load (Figure 6). In order to increase the reliability of the test results, each pile installed in identical soil conditions was subjected to the loading test at least twice. In case of a difference of less than 10% between repeated experiments, the average of them was taken; otherwise, an additional loading test were performed.

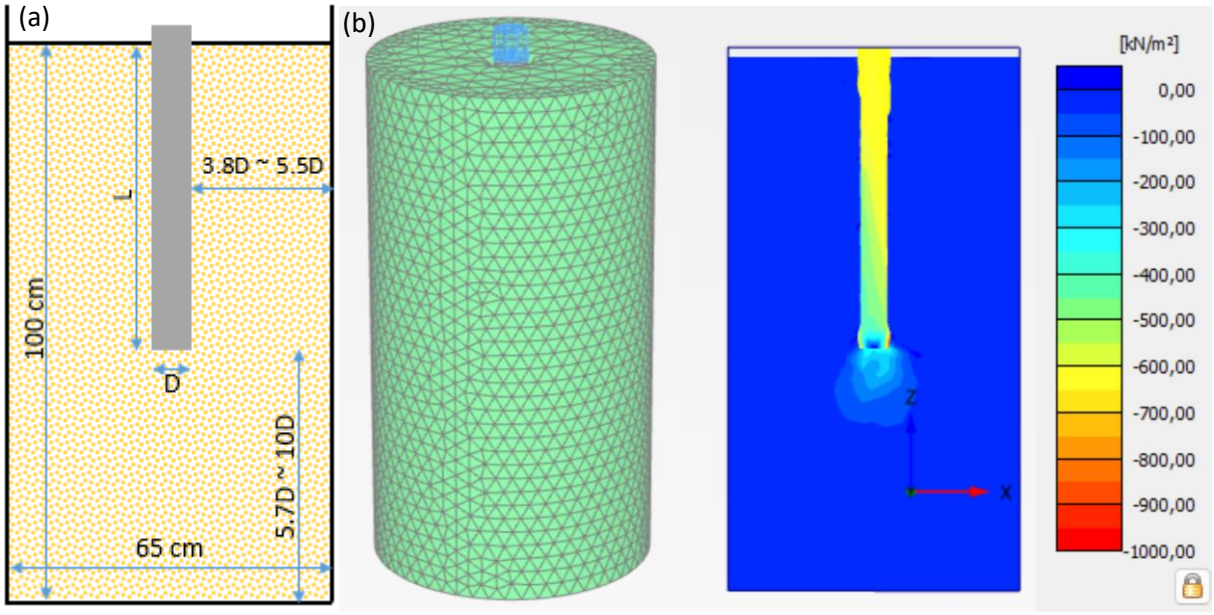

Figure 5. a) Experimental and b) numerical modelling of test pile in sand mass

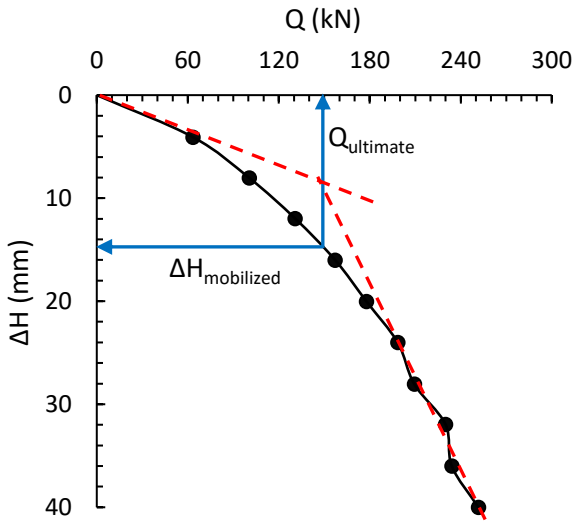

Figure 6. Application of tangent method

4. EXPERIMENTAL RESULTS

4.1 Effect of Loading Rate

Piles buried in dry and saturated soils were subjected to static loading. For this purpose, EN 1536:1999 [65] recommends the loading rate of piles as 1 mm/min, while ASTM D 1143-81 [66] suggests it as 1.25 mm/min. To examine the effect of loading rate on pile bearing capacity, the D70L600 pile was loaded at loading rates of 0.4-0.8-1.5-2.3-2.9-3.6-4.4-5.3-5.8 mm/min. According to the load-settlement curves (Q_p-ΔH, Q_u-ΔH), the rates of change in Q_p and Q_u values for different settlement amounts remained within the 6-10% level (Figure 7). This result shows that loading speed does not have a major effect on pile bearing capacity. Therefore, loading speed is 1.25 mm/min in pile loading tests.

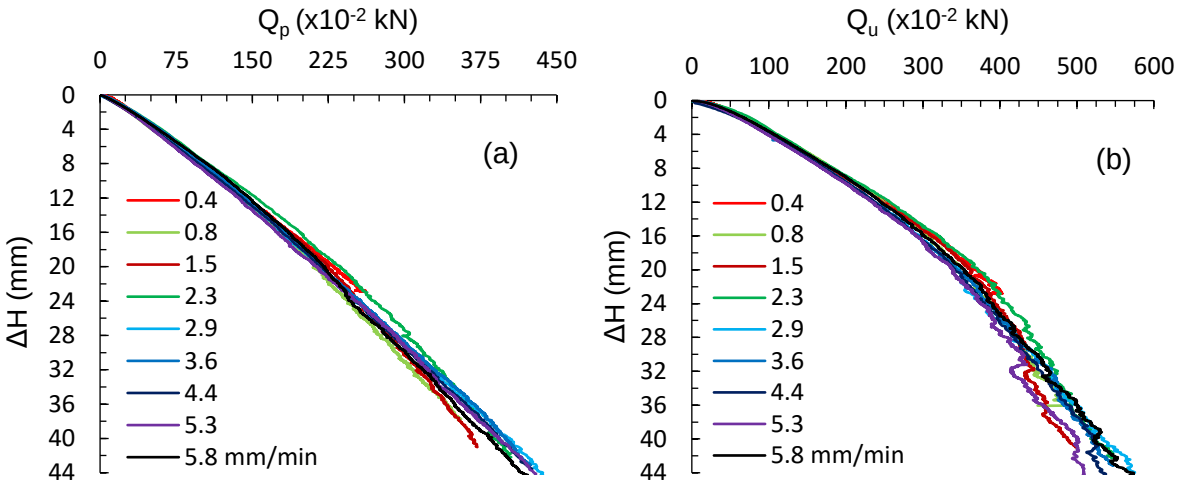

Figure 7. The load-settlement curves for D70L600 pile loaded in different loading speeds a) Q_p-ΔH curves, b) Q_u-ΔH curves

4.2 Pile Load Test Results

After the pile loading tests, the ultimate point and total bearing capacities of piles were determined by using the load-settlement curves given in Figure 8. The intersection points of tangent lines, which were drawn to the starting and ending portions of the load-settlement curves, was assumed to represent the ultimate bearing capacity of the pile [32] (Table 2). Ultimate bearing capacities of model piles were also calculated with analytical formulas (Equations 1-9). Theoretical ultimate base capacities of piles, using N_q coefficients developed by Janbu, Vesic, and Meyerhof, were calculated separately for each pile (Table 3 and Table 4).

In calculations made by existing theories, point capacities of piles are decreasing by 55.6%, 52.3%, and 60.8% according to methods of Janbu, Vesic, and Meyerhof, respectively, when soil changes from a dry state to a saturated state. The total bearing capacity reduce by 51.4 to 60.3% (Table 3 and Table 4). These reductions of the theoretical bearing capacities were not affected by the piles' geometry. K, tan δ, and N_q values used in formulas have fixed values depending on the internal friction angle of the soil (ϕ) having the same property. Therefore, pile point capacity increases linearly with depth depending on increment in effective stress. The internal friction angle of soil is modified by a few degrees since the saturation degree of the soil changes. However, change in ϕ does not affect the $K \cdot tan\,\delta$ value significantly. Due to the logarithmic increase in the value of N_q, changing a few degrees of ϕ affects the N_q value appreciably. However, the decrease in point capacity has been mostly caused by change in effective stress since the dry soil becomes saturated state. Pile loading test results show that the base capacities of piles decrease by 66.9 to 73.9% and 63.9 to 71.5% in total capacities when the dry soil becomes saturated (Table 2). In addition, decreasing amount of pile bearing capacity in the experiments is larger than the theory. Pile loading test results also reveal that variations on pile length and pile diameter affect reductions in pile bearing capacity proportionally.

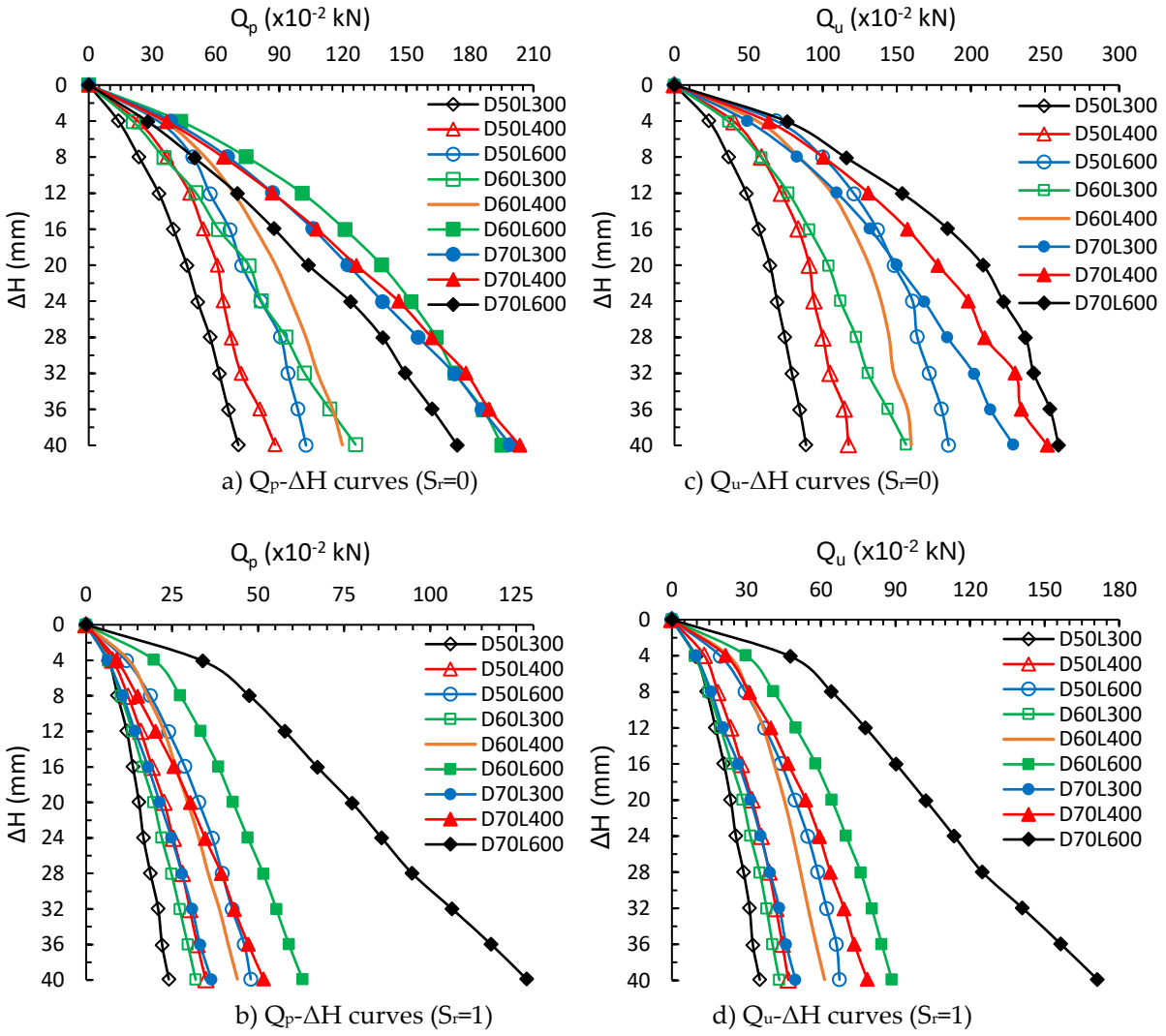

Figure 8. Load-settlement curves obtained from pile loading tests in dry (S_r=0) and saturated (S_r=1) sands

Table 2. Experimental results of ultimate bearing capacity values of the model piles in dry (S_r=0) and saturated (S_r=1) sandy soils

Piles	L/D	S_r=0				S_r=1			
		Q_p (kN)	ΔH (mm)	Q_u (kN)	ΔH (mm)	Q_p (kN)	ΔH (mm)	Q_u (kN)	ΔH (mm)
D70 L600	8.6	1.35	26.0	2.36	28.0	0.35	6.8	0.67	10.1
D70 L400	5.7	1.05	15.8	1.54	16.3	0.28	12.0	0.49	14.9
D70 L300	4.3	0.90	12.1	1.20	13.9	0.24	13.5	0.37	16.0
D60 L600	10.0	0.99	12.9	1.76	14.4	0.29	10.0	0.55	13.8
D60 L400	6.7	0.75	15.9	1.17	16.0	0.22	11.9	0.38	12.2
D60 L300	5.0	0.59	13.8	0.85	14.3	0.18	14.2	0.29	16.0
D50 L600	12.0	0.68	13.1	1.28	14.1	0.22	11.8	0.42	12.5
D50 L400	8.0	0.49	12.1	0.81	15.9	0.16	11.9	0.28	15.6
D50 L300	6.0	0.39	15.9	0.59	16.2	0.13	12.1	0.21	15.8

Table 3. Theoretical ultimate bearing capacity values of the model piles in dry soil (S_r=0)

Piles	Q_f (kN)	Q_p [a] (kN)			Q_u (kN)		
		Janbu	Vesic	Meyerhof	Janbu	Vesic	Meyerhof
D70 L600	0.20	1.68	3.92	4.05	1.88	4.12	4.25
D70 L400	0.09	1.12	2.61	2.70	1.21	2.70	2.79
D70 L300	0.05	0.84	1.96	2.02	0.89	2.01	2.07
D60 L600	0.17	1.24	2.88	2.97	1.41	3.05	3.14
D60 L400	0.07	0.82	1.92	1.98	0.89	1.99	2.05
D60 L300	0.04	0.62	1.44	1.49	0.66	1.48	1.53
D50 L600	0.14	0.86	2.00	2.06	1.00	2.14	2.20
D50 L400	0.06	0.57	1.33	1.38	0.63	1.39	1.44
D50 L300	0.04	0.43	1.00	1.03	0.47	1.04	1.07

[a] Nq values for ϕ=37.2° recommended by Janbu, Vesic, and Meyerhof are 44.5, 103.7, and 107, respectively. In the Janbu method, ψ is accepted as 90° at the pile base and in the Vesic method, I_{rr} is accepted as 100.

Table 4. Theoretical ultimate bearing capacity values of the model piles in saturated soil (S_r=1)

Piles	Q_f (kN)	Q_p [a] (kN)			Q_u (kN)		
		Janbu	Vesic	Meyerhof	Janbu	Vesic	Meyerhof
D70 L600	0.12	0.75	1.87	1.58	0.87	1.99	1.70
D70 L400	0.05	0.50	1.25	1.06	0.55	1.30	1.11
D70 L300	0.03	0.37	0.93	0.79	0.40	0.96	0.82
D60 L600	0.10	0.55	1.37	1.16	0.65	1.47	1.26
D60 L400	0.05	0.37	0.92	0.78	0.42	0.97	0.83
D60 L300	0.03	0.27	0.69	0.58	0.30	0.72	0.61
D50 L600	0.09	0.38	0.95	0.81	0.47	1.04	0.89
D50 L400	0.04	0.25	0.64	0.54	0.29	0.68	0.58
D50 L300	0.02	0.19	0.48	0.40	0.21	0.50	0.42

[a] Nq values for ϕ=34.5° recommended by Janbu, Vesic, and Meyerhof are 31.6, 79, and 67, respectively. In the Janbu method, ψ is accepted as 90° at the pile base and in the Vesic method, I_{rr} is accepted as 100.

Experimental results obtained in dry soil show that base capacity values of piles, according to the methods of Janbu, Vesic, and Meyerhof, were lower, by 0 to 20.8%, 54.1 to 66.0%, and 55.5 to 67.0%, respectively. The experimental ultimate load-bearing capacity of the piles was more than the method of Janbu at 25.4-34.9%, and less than the methods of Vesic and Meyerhof at 40-45% (Table 2 and Table 3). Experimental results obtained in saturated soil show that base capacity of piles was found lower by 32.8 to 52.9%, 73.1 to 81.2%, and 68.3 to 77.8% according to Janbu, Vesic, and Meyerhof, respectively. In terms of total capacity, according to Janbu, Vesic, and Meyerhof they were found lower, by 0.4 to 22.6%, 57.2 to 63.0%, and 50.0 to 60.6%, respectively (Table 3 and Table 4).

In general, base and total bearing capacity of piles installed in dry and saturated sands in the experiments were smaller than theoretical values. Dissimilarity in theoretical and experimental results discussed below.

4.2.1 Load-settlement behavior

The ultimate base and total capacities of single piles loaded in dry sands observed at the settlement levels of 12.1-26.0 mm and 13.9-28.0 mm, respectively. In saturated sand, the base and total capacities of piles mobilized at 6.8-14.2 mm and 10.1-16.0 mm settlement values (Table 2). The settlement values correspond to ultimate bearing capacity of pile, at the time of failure, are similar to Munaga et al. [67]. In the dry state, Q_p and Q_u were mobilized at normalized settlement values (ΔH/D) of 17.3-31.8% (average of 25%). In the saturated state, Q_p and Q_u were mobilized at normalized settlement values of 9.7-23.8% (average of 20%) and 14.4-31.6% (average of 24%), respectively (Figure 9). Shakeel and Ng [68] observed 2% normalized pile settlement (45-50 mm) at the working load of 0.75Q_u for large scale field tests (D=0.6m,

L=20m). Wang et al. [69] observed that piles, whose diameters of 1.5-1.8m and lengths of 52-83m, were mobilized at settlement values of 55.5-87.4 mm corresponding to 2.5-6.0% of pile diameter. The normalized settlement values obtained in the laboratory were greater than the pile loading test results in the field. This difference may be due to the geometry of the piles (L/D ratio) at laboratory and field scales. The L/D ratio of piles in the laboratory is at most 12, but this ratio can be 30-55 in the field. Depending on the pile length, vertical and horizontal stresses in the ground affect the settlement of the pile. On the other hand, the results obtained from this study were similar to other laboratory-scale studies since the piles have a diameter of 2.84 cm and a length of 25.3 cm reached their ultimate bearing capacity at 20-25% normalized settlement value [70].

In general, piles in the saturated sand reached their limit base and total capacities at lower settlement levels than piles in the dry sand. Moreover, Q_u is mobilized at greater settlement value than Q_p in the dry and saturated state. That is, each of the base and total capacities of piles reached their ultimate capacities at different settlement levels in dry and saturated sandy soils (Figure 9). Consequently, the pile shaft capacity mobilized at smaller settlement values than the base and total capacities. The use of different safety factors for shaft and base capacities to calculate the allowable bearing capacity may provide the opportunity to make a more economical design [71], [72]. TBEC [73] recommends using safety factors of 1.5 and 2.0 for ultimate shaft and base capacities of piles, respectively.

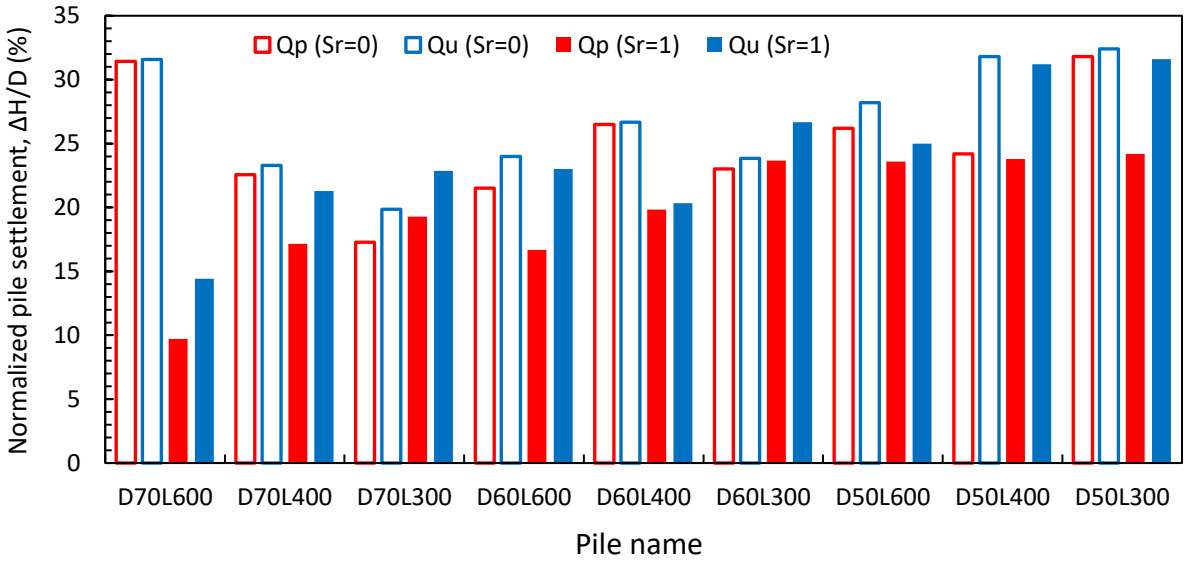

Figure 9. Normalized pile settlement values

A pile compresses the sandy soil under the pile bottom during the loading stage since settlement increases. Thus, the relative density and bearing capacity of soil under pile bottom increase. For this reason, point load-settlement curves of piles obtained from experiments exhibit quasi-linear behavior (Figure 8). Nevertheless, there is a point on the load-settlement curve at which the initial slope of the curve changes. In particular, piles installed in loose and medium dense sands exhibit similar behavior, and hence it is difficult to decide the ultimate base capacity of the pile in these soils [6], [54]. Compared with the piles in dry soils, the base capacities of piles in saturated sands reach their ultimate value at lower settlement values because the shear strength of saturated sand is less than dry sand having same relative density. In addition, the soil under the pile bottom moves more freely in vertical and lateral directions in saturated sands, when compared with dry sands.

4.2.2 Point resistance

There are differences between the experimental and theoretical results in pile base and total capacities. In the theoretical calculations, pile base capacities are 86 to 97.6% of the total bearing capacity in dry soil

and 81.5 to 97% in saturated soil. These results show that the pile point capacity constitutes a considerable part of the total load [9], [10], [32]. In the experimental results, the ratio of pile base capacity in the total bearing capacity represents 53 to 75% in dry soil, and 52 to 64% in saturated soil (Figure 10). Experimental results are closer to the load transfer mechanism of friction piles than theoretical results. The coefficients used to calculate the bearing capacity of the pile lead to the difference between experimental and theoretical results. Moreover, pile base capacity decreases if the L/D ratio increases (Figure 10). The same result was observed by Li et al. [74] in model pile loading experiments in sandy soils.

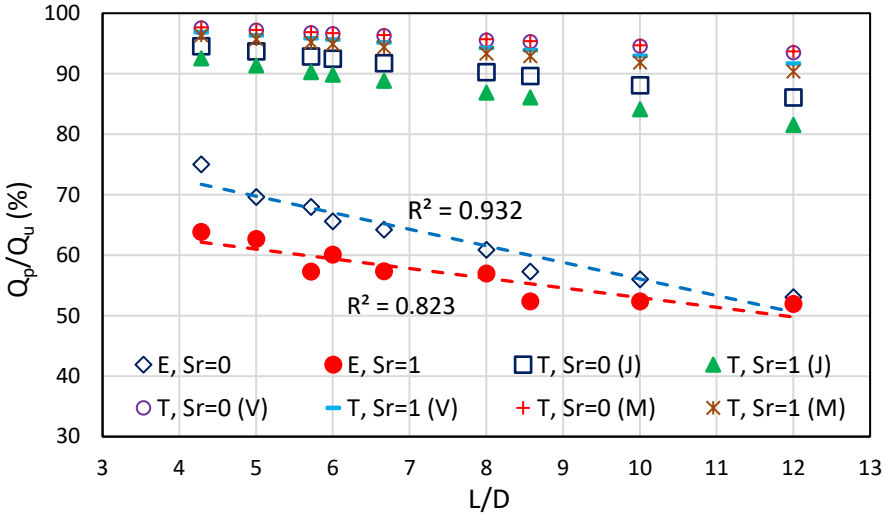

Figure 10. The percentage of point capacity in ultimate bearing capacity (E: experimental, T: theoretical, J: Janbu, V: Vesic, M: Meyerhof)

In theoretical methods, only the internal friction angle of the soil and the effective stress are considered while calculating the pile point resistance. However, the test results revealed that the diameter of the pile also affects the pile point resistance. In dry sands, the point resistance of same length piles decreases when L/D increases. That is, the point resistance increases when the pile diameter increases for piles having the same length (Figure 11). The contact area between soil particles and the pile bottom increases since the pile diameter increases. Therefore, point resistance increases. In saturated sands, for piles having the same length, the point resistance decreases as the pile diameter increases (when L/D decreases) (Figure 11). This is caused by the pore water pressure at the depth of pile base because a wider area is influenced by pore pressure.

The most important parameter affecting pile point resistance is the N_q value. In theory, N_q values vary depending on the ϕ of the soil. However, according to the test results, as the length of the same diameter piles in dry and saturated soil increases, the N_q values decrease (Figure 12). Since the L/D ratio increases, the shaft resistance of the pile increases and the load transferred to the pile end decreases (Figure 10). For the same length piles, increments of N_q values are the same with increments of point resistance if pile diameter increases. It is concluded that the N_q value is affected by pile geometry (L, D), saturation degree of soil (S_r), and effective stress (σ'). In addition, API [75] and CGS [76] recommend taking N_q values in the range of 12-40 and 30-60, respectively, for piles installed in medium dense sand. Experimental N_q values valid for dry sands are in good agreement with CGS [76]. N_q values recommended by API [75] are more representative of experimental N_q values obtained from the saturated state.

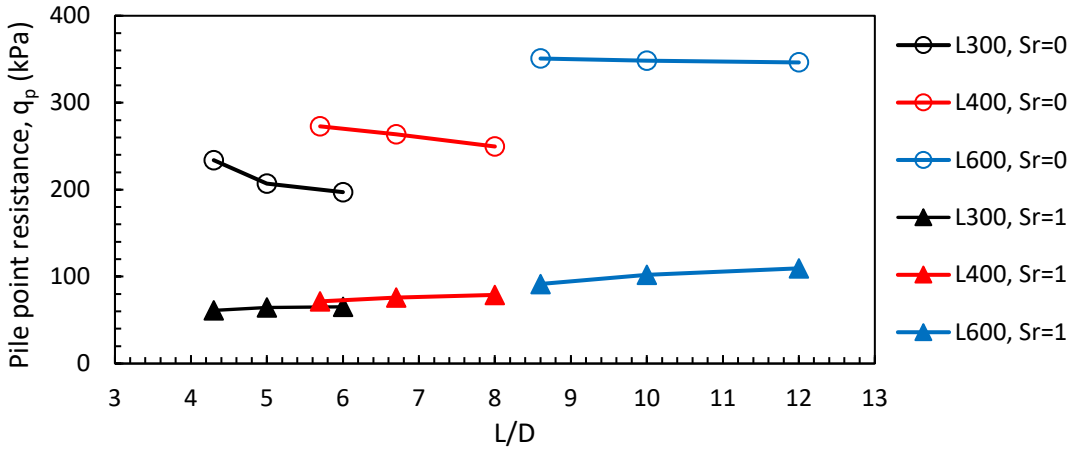

Figure 11. The variation of unit point resistance depending on L/D (modified from Yenginar et al. [54])

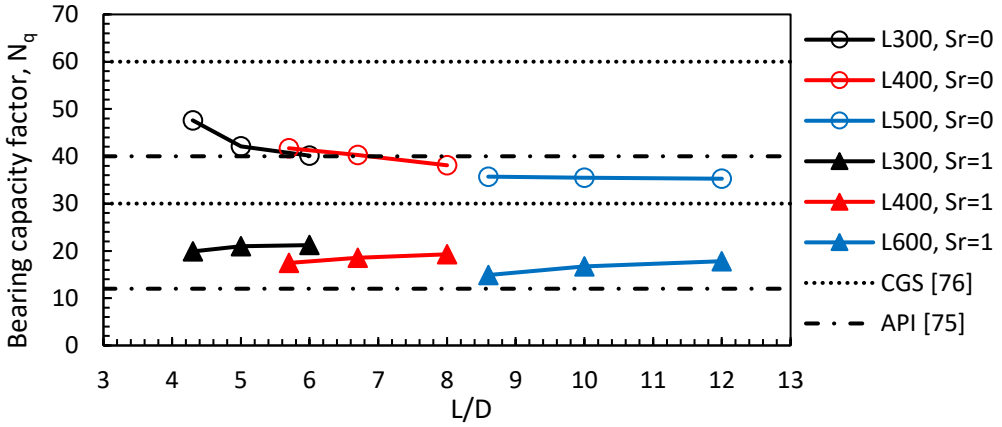

Figure 12. The variation of Nq values depending on L/D (modified from Yenginar et al. [54])

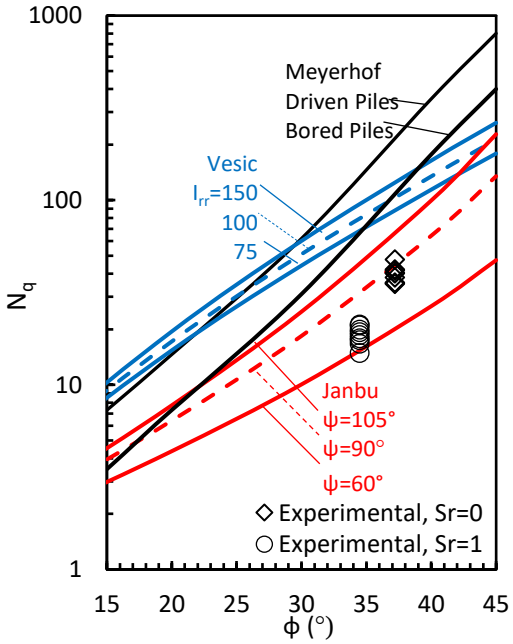

Figure 13. Theoretical and experimental N_q values depending on internal frictional angle (modified from Yenginar et al. [54])

Other than Janbu and Vesic, graphical charts presenting the variation in N_q values depending on ϕ have been developed by some researchers [28], [29], [31], [32]. In these curves, N_q values vary in a wide range even if the ϕ value is constant (Figure 13). For instance, the N_q values change between 10 and 60 for ϕ=30° while they vary between 30 and 180 for ϕ=40°. Field loading test results of piles installed in sandy soils having ϕ of 32-40° reveal that N_q values changes between 30 and 150 [77]. In this study, experimental N_q values are smaller than the Meyerhof and Vesic coefficients, and they are within the boundaries of Janbu (Figure 13).

5. CONCLUSION

In the present study, the load-settlement behavior of model piles was investigated with laboratory pile loading tests performed in dry (S_r=0) and saturated (S_r=1) sandy soils. The main findings of the study are given below.

- Loading speed during pile load test does not affect the ultimate point and total bearing capacities of the pile installed in sandy soils significantly.
- In saturated and dry sandy soils, ultimate values of the base, shaft, and total bearing capacities mobilized at different settlement values. Therefore, using different safety factors for base and shaft capacities is recommended to determine the allowable bearing capacity of piles.
- Total and base bearing capacities approximately decrease by 50 to 60% in theory when dry soil becomes saturated. In the pile loading test results, however, it is concluded that the reduction in base and total capacities of piles was 65 to 75% when the dry soil becomes saturated. The bearing capacity of the piled foundations will decrease more than expected since the groundwater level increase. In theory, the reason of the decrease in the bearing capacity is only decreasing amount of effective stress, but experimental results indicate that diameter of pile has also an influence in this reduction.
- Experimental N_q values are smaller than the Meyerhof and Vesic coefficients, and they are within the boundaries of Janbu. Thus, the authors recommend using Janbu's bearing capacity coefficients for medium-dense sandy soils.
- N_q values change depending on the effective stress, pile diameter, and saturation degree of soil. Defining the N_q value depending only on the internal friction angle of soil (ϕ) could be misleading.
- In dry and saturated sands, N_q value decreases since the pile length/pile diameter ratio increases.

The authors made some criticisms about the N_q parameter in the light of the pile loading test results obtained in the laboratory. The fact that the N_q values vary over a wide range and this makes it difficult to know the actual value, especially in the calculation of the pile base capacity. If the actual value of N_q can be determined more precisely using the pile and soil properties, the pile bearing capacity can be determined more accurately in the preliminary design. The results obtained in the study are valid for nondisplacement piles ($L/D \leq 12$), which are installed in medium dense sand in dry and saturated conditions. For this reason, new relationships based on pile and soil parameters can be developed for the N_q parameter by continuing experimental studies on the piles with different geometries (for practical concern, $L/D > 20$) constructed in soils having different grain distributions, relative density, and saturation degree.

Declaration of Ethical Standards

The authors declare that they comply with all ethical standards.

Credit Authorship Contribution Statement

Author 1: Resources, Investigation, Experimentation, Formal analysis, Validation, Methodology, Visualization, Writing – original draft **Author 2:** Resources, Investigation, Experimentation, Writing – original draft **Author 3:** Investigation, Validation, Methodology, Reviewing - original draft

Declaration of Competing Interest

The authors have no competing interests to declare that are relevant to the content of this article.

Funding / Acknowledgements

No funding information is available.

Data Avaibility

All data generated or analyzed during this study are included in this published article.

REFERENCES

[1] C. Cakiroglu, K. Islam, G. Bekdaş, and M. L. Nehdi, "Data-driven ensemble learning approach for optimal design of cantilever soldier pile retaining walls," *Structures*, vol. 51, pp. 1268–1280, May 2023, doi: 10.1016/j.istruc.2023.03.109.

[2] G. Bekdaş, Z. A. Arama, A. E. Kayabekir, and Z. W. Geem, "Optimal Design of Cantilever Soldier Pile Retaining Walls Embedded in Frictional Soils with Harmony Search Algorithm," *Applied Sciences*, vol. 10, no. 9, p. 3232, May 2020, doi: 10.3390/app10093232.

[3] H. Bolouri Bazaz, A. Akhtarpour, and A. Karamodin, "A study on the effects of piled-raft foundations on the seismic response of a high rise building resting on clayey soil," *Soil Dynamics and Earthquake Engineering*, vol. 145, p. 106712, Jun. 2021, doi: 10.1016/j.soildyn.2021.106712.

[4] I. Jamil *et al.*, "Analysis and Design of Piled Raft Foundation Taking into Account Interaction Factors," *Advances in Civil Engineering*, vol. 2022, pp. 1–11, Mar. 2022, doi: 10.1155/2022/1334136.

[5] R. Zhu *et al.*, "Improving the Performance of Piled Raft Foundations Using Deformation Adjustors: A Case Study," *Buildings*, vol. 12, no. 11, p. 1903, Nov. 2022, doi: 10.3390/buildings12111903.

[6] Y. Yenginar, "Investigation of group effect with model piled foundations [in Turkish]," Selcuk University, Institute of Science and Technology, Konya, Turkey, 2014.

[7] H. Bolouri Bazaz, A. Akhtarpour, and A. Karamodin, "A study on the effects of piled-raft foundations on the seismic response of a high rise building resting on clayey soil," *Soil Dynamics and Earthquake Engineering*, vol. 145, p. 106712, Jun. 2021, doi: 10.1016/j.soildyn.2021.106712.

[8] E. E. Başar, İ. D. Çelik, M. Fındık, and S. Uzundurukan, "Kohezyonsuz Zeminde Kazık Aralığının Belirlenmesi ve Temel Davranışının Deneysel İncelenmesi," *Turkish Journal of Civil Engineering*, vol. 34, no. 2, pp. 145–172, Mar. 2023, doi: 10.18400/tjce.1244594.

[9] J. E. Bowles, *Foundation analysis and design*. McGraw-Hill Book Company, NY, 1997.

[10] B. M. Das, *Principles of foundation engineering*. Thomson Canada Limited, Canada, 2007.

[11] S. Manandhar and N. Yasufuku, "Analytical Model for the End-Bearing Capacity of Tapered Piles Using Cavity Expansion Theory," *Advances in Civil Engineering*, vol. 2012, pp. 1–9, 2012, doi: 10.1155/2012/749540.

[12] N. Miura, "Point resistance of piles in sand," *Technology reports of the Yamaguchi University*, vol. 3, no. 2, pp. 129–139, 1983.

[13] S. Ohno and S. Sawada, "Bearing capacity of piles in sands with different crushabilities under various stress conditions," in *Proceeding 11th Asian Regional Conf on Soil Mechanics and Geotech Eng*,

1999, pp. 249–252.
[14] N. Yasufuku and A. F. L. Hyde, "Pile end-bearing capacity in crushable sands," *Géotechnique*, vol. 45, no. 4, pp. 663–676, Dec. 1995, doi: 10.1680/geot.1995.45.4.663.
[15] Q. Zhang, Z. Zhang, and S. Li, "Investigation into Skin Friction of Bored Pile Including Influence of Soil Strength at Pile Base," *Marine Georesources & Geotechnology*, vol. 31, no. 1, pp. 1–16, Jan. 2013, doi: 10.1080/1064119X.2011.626506.
[16] Z. Jia-Jin, G. Xiao-Nan, Z. Ri-Hong, W. Kui-Hua, and Y. Tian-Long, "Shaft capacity of pre-bored grouted planted nodular pile under various overburden pressures in dense sand," *Marine Georesources & Geotechnology*, vol. 38, no. 1, pp. 97–107, Jan. 2020, doi: 10.1080/1064119X.2018.1553214.
[17] A. Mishra and V. A. Sawant, "Optimization of Empirical Methods in Determining the Load Capacity of Rock Socketed Piles," *Indian Geotechnical Journal*, vol. 52, no. 4, pp. 852–864, Aug. 2022, doi: 10.1007/s40098-022-00629-9.
[18] E. C. Junior and A. S. Moura, "Evaluation of the Group Effect's Simulation on the Bearing Capacity of Bored Piles in Granular Soil, Using Load Transfer Functions," *Geotechnical and Geological Engineering*, vol. 40, no. 7, pp. 3393–3412, Jul. 2022, doi: 10.1007/s10706-022-02100-1.
[19] R. Wang, D. E. L. Ong, J. Zhou, S. Liu, and E. Oh, "Validation of Analytical Solutions for Predicting Drilled Pile Behaviour under Bi-Directional Static Load Tests," *Geosciences (Basel)*, vol. 12, no. 8, p. 284, Jul. 2022, doi: 10.3390/geosciences12080284.
[20] E. M. Comodromos and M. F. Randolph, "Improved Relationships for the Pile Base Response in Sandy Soils," *Journal of Geotechnical and Geoenvironmental Engineering*, vol. 149, no. 8, Aug. 2023, doi: 10.1061/JGGEFK.GTENG-11035.
[21] G. Cao, X. Ding, Z. Yin, H. Zhou, and P. Zhou, "A new soil reaction model for large-diameter monopiles in clay," *Comput Geotech*, vol. 137, p. 104311, Sep. 2021, doi: 10.1016/j.compgeo.2021.104311.
[22] Y. Zhang *et al.*, "A new approach for estimating the vertical elastic settlement of a single pile based on the fictitious soil pile model," *Comput Geotech*, vol. 134, p. 104100, Jun. 2021, doi: 10.1016/j.compgeo.2021.104100.
[23] T. A. Pham and M. Sutman, "A Simplified Method for Bearing-Capacity Analysis of Energy Piles Integrating Temperature-Dependent Model of Soil–Water Characteristic Curve," *Journal of Geotechnical and Geoenvironmental Engineering*, vol. 149, no. 9, Sep. 2023, doi: 10.1061/JGGEFK.GTENG-11095.
[24] X.-Y. Li, J.-H. Wan, H.-P. Zhao, and S.-W. Liu, "Three-Dimensional Analysis of Nonlinear Pile–Soil Interaction Responses Using 3D Pile Element Model," *International Journal of Geomechanics*, vol. 21, no. 8, Aug. 2021, doi: 10.1061/(ASCE)GM.1943-5622.0002076.
[25] X. Zhang, B. Jiao, and B. Hou, "Reliability analysis of horizontally loaded pile considering spatial variability of soil parameters," *Soil Dynamics and Earthquake Engineering*, vol. 143, p. 106648, Apr. 2021, doi: 10.1016/j.soildyn.2021.106648.
[26] A. Akbari Garakani, B. Heidari, S. Mokhtari Jozani, and O. Ghasemi-Fare, "Numerical and Analytical Study on Axial Ultimate Bearing Capacity of Fixed-Head Energy Piles in Different Soils," *International Journal of Geomechanics*, vol. 22, no. 1, Jan. 2022, doi: 10.1061/(ASCE)GM.1943-5622.0002223.
[27] F. Han, R. odrigo Salgado, M. Prezzi, and J. Lim, "Shaft and base resistance of non-displacement piles in sand," *Comput Geotech*, vol. 83, pp. 184–197, Mar. 2017, doi: 10.1016/j.compgeo.2016.11.006.
[28] V. G. Berezantzev, "Load bearing capacity and deformation of piled foundations," in *Proceeding 5th Int Conf ISSMFE*, Paris, FR: ISSMFE, 1961, pp. 11–12.
[29] J. B. Hansen, "A general formula for bearing capacity. ," 1961.
[30] N. Janbu, "Static bearing capacity of friction piles," *J of Soil Mec. and Found Eng Div ASCE*, vol. 95, 1976.
[31] G. G. Meyerhof, " Bearing capacity and settlement of pile foundations," *J of Geotech Eng Div*, vol.

102, no. GT3, 1976.
[32] M. J. Tomlinson, *Foundation design and construction*. New York: John Willey and Sons, 1986.
[33] A. S. Vesic, *Design of pile foundations*. Washington, DC: Synthesis of Highway Practice 42 Res Bd, 1977.
[34] Y. M. Cheng, "Nq factor for pile foundations by Berezantzev," *Géotechnique*, vol. 54, no. 2, pp. 149–150, Mar. 2004, doi: 10.1680/geot.2004.54.2.149.
[35] H. G. Poulos and E. H. Davis, *Pile foundation analysis and design* . New York: John Willey and Sons, New York, 1980.
[36] F. H. Kulhawy, "Limiting tip and side resistance: fact or fallacy?," in *Proceeding Symp on Analysis and Design of Pile Foundations, ASCE*, 1984, pp. 80–98.
[37] W. J. Neely, "Bearing Capacity of Expanded-Base Piles in Sand," *Journal of Geotechnical Engineering*, vol. 116, no. 1, pp. 73–87, Jan. 1990, doi: 10.1061/(ASCE)0733-9410(1990)116:1(73).
[38] G. G. Meyerhof, "Scale Effects of Ultimate Pile Capacity," *Journal of Geotechnical Engineering*, vol. 109, no. 6, pp. 797–806, Jun. 1983, doi: 10.1061/(ASCE)0733-9410(1983)109:6(797).
[39] M. D. Bolton, "The strength and dilatancy of sands," *Géotechnique*, vol. 36, no. 1, pp. 65–78, Mar. 1986, doi: 10.1680/geot.1986.36.1.65.
[40] X. Jia, H. Zhang, C. Wang, F. Liang, and X. Chen, "Influence on the lateral response of offshore pile foundations of an asymmetric heart-shaped scour hole," *Applied Ocean Research*, vol. 133, p. 103485, Apr. 2023, doi: 10.1016/j.apor.2023.103485.
[41] K. Natarajan and G. S. P. Madabhushi, "Seismic response of an offshore wind turbine jacket structure with pile foundations," *Soil Dynamics and Earthquake Engineering*, vol. 162, p. 107427, Nov. 2022, doi: 10.1016/j.soildyn.2022.107427.
[42] Z. Xiao-ling, L. Cheng-rui, W. Pi-guang, and Z. Guo-liang, "Experimental simulation study on dynamic response of offshore wind power pile foundation under complex marine loadings," *Soil Dynamics and Earthquake Engineering*, vol. 156, p. 107232, May 2022, doi: 10.1016/j.soildyn.2022.107232.
[43] L. Wang and T. Ishihara, "A semi-analytical one-dimensional model for offshore pile foundations considering effects of pile diameter and aspect ratio," *Ocean Engineering*, vol. 250, p. 110874, Apr. 2022, doi: 10.1016/j.oceaneng.2022.110874.
[44] X. Wang, S. Li, and J. Li, "Effect of pile arrangement on lateral response of group-pile foundation for offshore wind turbines in sand," *Applied Ocean Research*, vol. 124, p. 103194, Jul. 2022, doi: 10.1016/j.apor.2022.103194.
[45] V. D. Nguyen, J. C. Small, and H. G. Poulos, "The Effects of Groundwater Pumping on Piled Foundations," in *Computational Mechanics–New Frontiers for the New Millennium*, Elsevier, 2001, pp. 433–438. doi: 10.1016/B978-0-08-043981-5.50067-5.
[46] M. Sheikhtaheri, " Experimental and numerical modeling studies for interpreting and estimating the p–δ behavior of single model piles in unsaturated sand ," University of Ottawa, Canada, 2014.
[47] M. Olgun, B. Fidan, and Y. Yenginar, "Model Studies of Lateral Soil Pressure on Drilling Piles in Dry and Saturated Sands," *Soil Mechanics and Foundation Engineering*, vol. 56, no. 4, pp. 280–286, Sep. 2019, doi: 10.1007/s11204-019-09603-9.
[48] M. Mukhlisin, B. Hamdani, E. Novita, S. Sukoyo, and A. H. Rabinah, "Behaviour of Friction Resistance of Pile Groups on Clay Soil During Loading Tests: Case Study in Semarang and Temanggung, Central Java, Indonesia," *Indonesian Journal on Geoscience*, vol. 9, no. 1, 2021, doi: 10.17014/ijog.9.1.61-69.
[49] H. Phoban, U. Seeboonruang, and P. Lueprasert, "Numerical Modeling of Single Pile Behaviors Due to Groundwater Level Rising," *Applied Sciences*, vol. 11, no. 13, p. 5782, Jun. 2021, doi: 10.3390/app11135782.
[50] Y. Roh, I. Kim, G. Kim, and J. Lee, "Comparative Analysis of Axial Load Capacity for Piled-Raft Foundation with Changes in Groundwater Level," *KSCE Journal of Civil Engineering*, vol. 23, no. 10, pp. 4250–4258, Oct. 2019, doi: 10.1007/s12205-019-0239-3.

[51] E. E.-M. Chong and D. E.-L. Ong, "Data-Driven Field Observational Method of a Contiguous Bored Pile Wall System Affected by Accidental Groundwater Drawdown," *Geosciences (Basel)*, vol. 10, no. 7, p. 268, Jul. 2020, doi: 10.3390/geosciences10070268.

[52] K. Amornfa, H. T. Quang, and T. V Tuan, "Effect of groundwater level change on piled raft foundation in Ho Chi Minh City, Viet Nam using 3D-FEM," *Geomech. Eng*, vol. 32, no. 4, pp. 387–396, 2023.

[53] T. L. Gia, L. T. Duy, T. D. T. Kieu, and H. N. Thu, "The impact of groundwater lowering on pile bearing capacity in Hanoi – Vietnam," 2020, pp. 137–144. doi: 10.1007/978-981-15-2184-3_17.

[54] Y. Yenginar, B. Fidan, and M. Olgun, "Experimental and theoretical Nq values for dry and saturated sands," in *4th International Conference on New Developments in Soil Mechanics and Geotechnical Engineering*, 2016, pp. 149–156.

[55] Gg. Meyerhof, "The bearing capacity of foundations under eccentric and inclined loads," in *Proc. of the 3rd Int. Conf. on SMFE*, 1953, pp. 440–445.

[56] B. M. Das and N. Sivakugan, *Principles of foundation engineering*. Cengage learning, 2018.

[57] D. NAVFAC, "Foundation and Earth Structures," *US Department of the Navy*, 1984.

[58] J. B. Burland, "Shaft friction piles in clay-a simple fundamental approach," *Ground Engineering*, vol. 3, pp. 30–42, 1973.

[59] ASTM D2487-17e1, "Standard practice for classification of soils for engineering purposes (Unified Soil Classification System)," in *Book of Standards Volume: 04.08*, ASTM International, West Conshohocken, PA, USA., 2020, pp. 1–10.

[60] ASTM D4254-16, "Standard test methods for minimum index density and unit weight of soils and calculation of relative density," in *Book of Standards Volume: 04.08*, 8th ed., vol. 4, West Conshohocken, PA: ASTM International, 2016, pp. 1–9.

[61] C. Tang, R. H. Borden, and M. A. Gabr, "A Simplified Direct Shear Testing Procedure to Evaluate Unsaturated Shear Strength," *Geotechnical Testing Journal*, vol. 41, no. 2, p. 20150161, Mar. 2018, doi: 10.1520/GTJ20150161.

[62] ASTM D1143, "Standard Test Methods for Deep Foundations Under Static Axial Compressive Load," in *Book of Standards*, West Conshohocken, PA, USA: ASTM International, 2013.

[63] J. M. O. Hughes, N. J. Withers, and D. A. Greenwood, "A field trial of the reinforcing effect of a stone column in soil," *Géotechnique*, vol. 25, no. 1, pp. 31–44, Mar. 1975, doi: 10.1680/geot.1975.25.1.31.

[64] US Army Corps of Engineers, "EL 02 CO97," US Army Publication, USA, 1997.

[65] EN:1536, "Execution of special geotechnical work-bored piles," 1999.

[66] ASTM D1143, "Standard Test Methods for Deep Foundations Under Static Axial Compressive Load," in *Book of Standards*, West Conshohocken, PA, USA: ASTM International, 2013.

[67] T. Munaga, M. M. Khan, and K. K. Gonavaram, "Axial and Lateral Loading Behaviour of Pervious Concrete Pile," *Indian Geotechnical Journal*, vol. 50, no. 3, pp. 505–513, Jun. 2020, doi: 10.1007/s40098-019-00377-3.

[68] M. Shakeel and C. W. W. Ng, "Settlement and load transfer mechanism of a pile group adjacent to a deep excavation in soft clay," *Comput Geotech*, vol. 96, pp. 55–72, Apr. 2018, doi: 10.1016/j.compgeo.2017.10.010.

[69] P. Wang, H. Ding, J. Zhou, W. Hu, X. Gu, and E. Oh, "Field Tests of Super-Long and Large-Diameter Drilled Shaft Pile Foundations," *Advances in Civil Engineering*, vol. 2020, pp. 1–12, Jun. 2020, doi: 10.1155/2020/8814257.

[70] M. Sharafkhah and I. Shooshpasha, "Physical modeling of behaviors of cast-in-place concrete piled raft compared to free-standing pile group in sand," *Journal of Rock Mechanics and Geotechnical Engineering*, vol. 10, no. 4, pp. 703–716, Aug. 2018, doi: 10.1016/j.jrmge.2017.12.007.

[71] V. N. S. Murthy, *Advanced foundation engineering.* . New Delhi, India: CBS Publishers and Distributors, 2007.

[72] Y. Yenginar and Ö. Tan, "Kumlu Zeminlerdeki Tekil Kazığın Eksenel Yük Altındaki Yük-Oturma

Davranışının Model Deneylerle Araştırılması," in *6. Geoteknik Sempozyumu*, 2015.

[73] TBEC, "Turkish building earthquake code," Disaster and Emergency Management Authority (AFAD), Ankara, Turkey, 2019.

[74] Y. Li, C. Liu, and J. Song, "The Pile End Mechanism of Jacked Pile in Layered Soils," *Indian Geotechnical Journal*, vol. 51, no. 5, pp. 1087–1098, Oct. 2021, doi: 10.1007/s40098-021-00510-1.

[75] API (American Petroleum Institute), "Planning, designing and constructing fixed offshore platforms — Working stress design," API Recommended Practice 2A-WSD (RP 2A-WSD). Washington, DC:API, 2003.

[76] CGS (Canadian Geotechnical Society), "Canadian foundation engineering manual," 4th ed. Alberta, Canada: CGS, 2006.

[77] B. H. Fellenius, *Basics of foundation design*, Electronic Edition. Sidney, British Columbia, Canada: See www.Fellenius.net., 2015.